Device-Free Presence Detection and Localization With SVM and CSI Fingerprinting

Rui Zhou, *Member, IEEE*, Xiang Lu, Pengbiao Zhao, and Jiesong Chen

Abstract—Presence detection and localization are of importance to a variety of applications. Most previous approaches require the objects to carry electronic devices, while on many occasions device-free presence detection and localization are in need. This paper proposes a device-free presence detection and localization algorithm based on WiFi channel state information (CSI) and support vector machines (SVM). In the area of interest covered with WiFi, human movements may cause observable alteration of WiFi signals. By analyzing the CSI fingerprint patterns, the proposed algorithm is able to detect human presence through SVM classification. By establishing the nonlinear relationship between CSI fingerprints and locations through SVM regression, the proposed algorithm is able to estimate the object locations according to the measured CSI fingerprints. To cope with the noisy WiFi channels, the proposed algorithm applies density-based spatial clustering of applications with noise to reduce the noise in CSI fingerprints, and applies principal component analysis to extract the most contributing features and reduce the dimensionality of CSI fingerprints. Evaluations in two typical scenarios achieved the presence detection precision of over 97%, and the localization accuracy of 1.22 and 1.39 m, respectively.

Index Terms—Channel state information (CSI), device-free, localization, presence detection, support vector machine (SVM).

I. INTRODUCTION

PRESENCE detection and localization have been the focus of research for years. A common solution to these problems is to pinpoint mobile devices in a WiFi infrastructure. Such a solution requires the active participation of mobile devices. However, on many occasions, such as at home or in sensitive areas, the objects may not carry any electronic devices or power them off. Thus, device-free presence detection and localization are in need, which detect and track the objects that do not carry any electronic devices nor participate actively in the process. Approaches to device-free presence detection and localization include radar based systems and vision based systems. These systems, however, require specialized hardware and high cost. As WiFi networks are widely deployed, device-free presence detection and localization based on WiFi infrastructure have attracted much attention recently. Researches [1] show that Received Signal Strength

Indication (RSSI) can be used to achieve device-free presence detection and localization, as RSSI is affected by human movements. However, changes in indoor environments and multipath fading cause instability and declining of detection and localization accuracy.

Channel State Information (CSI) is a fine-grained measurement from the physical layer which describes the amplitude and phase of each orthogonal subcarrier in a channel. Researches [2], [3] show that WiFi CSI is more temporally stable and provides the capability to benefit from the multipath effect, thus suitable for accurate presence detection and localization. Several researches have been conducted in the field of presence detection [4]–[7] and localization in a device-based [1], [3], [8] or device-free [2], [9]–[12] manner. Novel applications based on CSI are emerging as well, such as activity recognition [13], [14], fall detection [15], [16], gesture recognition [17], human identification [18] and crowd counting [19], [20].

Previous work on CSI-based localization mainly used signal propagation models [1], [10], fingerprinting with Bayesian approaches [2], [3], or fingerprinting with classification approaches [8], [9]. Due to the complexity of indoor environments, it is difficult to establish accurate signal propagation models, hence CSI fingerprinting outperforms propagation models [3]. Fingerprinting with Bayesian approaches and classification approaches treat localization as discrete problems, while localization is a continuous problem estimating the coordinates, which can be solved by regression. Previous work on CSI-based presence detection focused mainly on moving human [6], [7] or used different methods to detect moving and stationary human separately [5]. Observations show that CSI exhibits different patterns between human presence and vacancy, thus presence detection can be treated as binary classification regardless of human moving or stationary.

In this paper, we treat device-free presence detection as a classification problem, and treat device-free localization as a regression problem [21] by establishing the nonlinear relationship between locations and CSI fingerprints using empirical data without considering the complex environment. We propose to apply Support Vector Machines (SVM) on WiFi CSI to achieve presence detection and localization. The process goes through CSI data collection, feature extraction, model training to establish the presence detection classifier and the relationship between CSI fingerprints and locations, and classification to detect presence or regression to estimate locations, as illustrated in Fig. 1. Human presence is a prerequisite to localization. To deal with the noisy WiFi channels, we propose
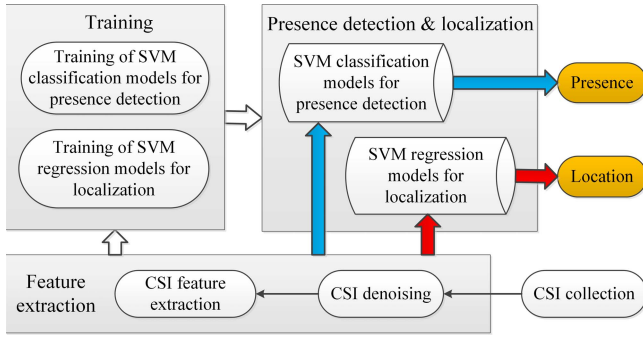
Fig. 1.   The algorithm of device-free presence detection and localization.

to apply Density-Based Spatial Clustering of Applications with Noise (DBSCAN) on the CSI data to reduce noise. To reduce the dimensionality of CSI fingerprints and thus reduce computing complexity, we propose to apply Principal Component Analysis (PCA) to extract the most contributing features from the CSI data. Evaluations in two typical testbeds achieved the localization accuracy of 1.22 m and 1.39 m, and presence detection precision of more than 97%. The main contributions of the paper are as follows:

1) Apply SVM classification to perform device-free presence detection regardless of human moving or stationary;
2) Apply SVM regression to perform device-free localization, by modelling the nonlinear relationship between CSI fingerprints and locations without considering the complex indoor environment;
3) Apply DBSCAN to reduce noise in CSI data;
4) Apply PCA to extract the most contributing features from CSI data and reduce the dimensionality;
5) Regarding the performance of presence detection, compare CSI with RSSI, compare PCA with other feature extraction methods, compare SVM classification with Bayesian;
6) Regarding the performance of localization, compare CSI with RSSI, compare SVM regression with SVM classification and Bayesian, compare our solution with other existing solutions;
7) Investigate the parameters that affect the performance of presence detection and localization, such as number of access points, number of antennas, sampling density, and PCA cumulative contribution.

The rest of the paper is organized as follows. Section II reviews the related work briefly. Section III presents the CSI data collection and feature extraction process. Section IV proposes the device-free presence detection and localization algorithm with SVM. Evaluations, comparisons and analyses are reported in Section V. Section VI concludes the paper.

II. RELATED WORK

A. Localization With CSI

The FILA [1] system was claimed to be the first to use CSI for device-based indoor localization. It developed a refined indoor propagation model representing the relationship between CSI values and distance and applied trilateration to accomplish localization. Wu *et al.* [3] extended the FILA system with a CSI-based fingerprinting approach using maximum likelihood algorithm, achieving an improved accuracy. Abdel-Nasser *et al.* [2] introduced MonoPHY as a single stream device-free localization system, which used a cluster-based CSI fingerprinting approach with maximum likelihood algorithm. MonoStream [9] enhanced MonoPHY and modelled the device-free localization problem as an object recognition problem and extracted features that could capture small variations in the effect of human standing at different locations on the CSI vectors. Wang *et al.* [8] presented a device-based indoor fingerprinting system (DeepFi) using CSI. Deep learning was utilized to train all the weights of a deep network as fingerprints and a Bayesian probabilistic method based on Radial Basis Function (RBF) was used to obtain the estimated location. To mitigate the issue of prior training, LiFS [10] estimated the locations by modelling the CSI measurements of multiple wireless links as a set of power fading based equations and only the subcarriers affected by multipath were utilized for localization. By detecting the subtle reflection signals from human body and further differentiating them from those reflected signals from static objects, MaTrack [11] identified the human target's angle and tracked walking human without prior training as well. Qian *et al.* [12] proposed Widar that simultaneously estimated human moving velocities (i.e. speed and direction) and locations by modelling the relationships between CSI dynamics and locations and velocities without prior training.

B. Presence Detection With CSI

Zhou *et al.* [4] used a deterministic CSI fingerprinting method and a threshold-based method separately to detect human presence in an omnidirectional manner. Wu *et al.* [5] proposed DeMan for device-free detection of moving and stationary human. DeMan took advantage of amplitude and phase information of CSI to detect moving human and considered human breathing as an intrinsic indicator of stationary human presence. Lv *et al.* [6] proposed speed independent device-free entity detection (SIED) suitable for intrusion detection of different entity moving speeds. SIED captured the variance of variances of amplitudes of each CSI subcarrier and combined Hidden Markov Model (HMM) to make entity detection a probability problem. Zhu *et al.* [7] proposed R-TTWD for device-free through-the-wall detection of moving human by taking advantage of the correlated changes over different subcarriers and extracting the first-order difference of eigenvector of CSI amplitudes across different subcarriers.

C. Emerging Novel Applications Based on CSI

Wang *et al.* [13] presented device-free location-oriented activity identification at home through the use of CSI. Qian *et al.* [14] derived motion-induced Doppler shifts using CSI, and extracted motion directions for exergame designs. Han *et al.* [15] proposed a passive fall detection method (WiFall) based on time variability and special diversity of CSI. Wang *et al.* [16] presented a more accurate indoor fall
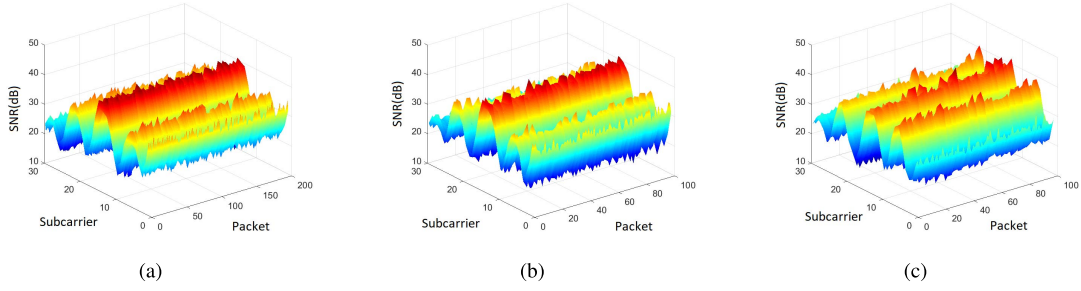
Fig. 2. CSI exhibits different patterns when no human is present or a human is at different locations. (a) No human. (b) Human at location 1. (c) Human at location 2.

detection system (RT-Fall), exploiting the phase and amplitude of CSI. Taking advantage of the patterns of CSI in the time series that are generated by finger moves, WiFinger [17] could recognize a set of finger-grained gestures. Wang *et al.* [18] proposed WiFiU to capture fine-grained gait patterns using CSI to identify humans, which generated spectrograms from CSI measurements and extracted features from spectrograms. Xi *et al.* [19] presented device-free crowd counting (Electronic Frog Eye) based on CSI by formulating the monotonic relationship between the crowd number and various features of CSI by the Grey Verhulst Model. Domenico *et al.* [20] presented a device-free crowd counting and occupancy estimation system by analyzing the shape of the Doppler spectrum of the received signal which was correlated to the number of people moving in the monitored environment.

III. CSI COLLECTION AND FEATURE EXTRACTION

The infrastructure of presence detection and localization is composed of wireless Access Points (AP) for data transmission, Monitoring Points (MP) for data retrieval, and a server for data processing. The APs can be commodity wireless routers supporting 802.11n, i.e. supporting Orthogonal Frequency Division Multiplexing (OFDM) and Multiple-Input Multiple-Output (MIMO). The MPs are commodity wireless adapters supporting 802.11n, with modified firmware and driver to retrieve CSI [22], [23]. For complete coverage of the area of interest, each pair of AP-MP is placed at corners or edges, forming diagonal lines. Each pair of transmitting-receiving antennas (a TX-RX pair) is a link.

CSI is fine-grained information from the physical layer that describes Channel Frequency Response (CFR) from the transmitter to the receiver. Leveraging commodity Network Interface Card (NIC) with modified firmware and driver [22], [23], the amplitude and phase of each subcarrier within a channel can be revealed to the upper layers for each packet in the format of CSI. The raw data collected contain the number of transmitting antennas N_{tx}, the number of receiving antennas N_{rx}, packet transmission frequency f, and CSI matrix H, which is a $N_{tx} \times N_{rx} \times N$ matrix:

$$H = (H_{ij})_{N_{tx} \times N_{rx}} \tag{1}$$

H_{ij} is the CSI of the link formed by TX i and RX j, containing the information of N subcarriers, expressed as

$$H_{ij} = (h_1, h_2, \cdots, h_N)^T, \quad i \in [1, N_{tx}], \ j \in [1, N_{rx}] \tag{2}$$

The k-th subcarrier in H_{ij} can be expressed as

$$h_k = |h_k|e^{j\angle h_k}, \quad k \in [1, N] \tag{3}$$

where $|h_k|$ is the amplitude response and $\angle h_k$ is the phase response of subcarrier k.

We use Signal-to-Noise Ratio (SNR) to represent amplitude in the following processing. SNR is defined as the ratio of signal power to noise power, often expressed in decibels (dB). In the CSI matrix, h_k is a complex number. It is firstly converted to its magnitude $|h_k|$, which is in voltage space and converted to SNR in power space by the function

$$SNR_k = 10log_{10}(|h_k|^2) \tag{4}$$

Due to slight frequency delta, separate subcarriers experience different multipath fading. When small movements have altered the environment, the individual subcarrier measurements are more likely to change. CSI portrays a fine-grained temporal and spectral structure of wireless links and exhibits properties suitable for presence detection and localization.

1) Presence detection: CSI exhibits different patterns when the area of interest is vacant or a human appears. Fig. 2 illustrates the properties of CSI of one link for device-free presence detection, in which the packet-axis represents the packets over time, the subcarrier-axis represents each subcarrier in the link, and the SNR-axis represents the amplitude of each subcarrier. Different colors represent different amplitude levels. Fig. 2(a) illustrates the amplitude of each subcarrier in the link over time/packets when no human is present in the area of interest. Its pattern is quite different from the CSI patterns when a human appears, as Fig. 2(b) and Fig. 2(c) show. Human presence can be detected through classification on CSI patterns.

2) Localization: CSI also exhibits differences when a human is at different locations. Fig. 2(b) and Fig. 2(c) show the amplitude of subcarriers in one link over time/packets when a human stands at two locations 1 m apart. The CSI patterns have obvious variations between them. Such properties of CSI indicate that there are certain relationships between CSI values and locations, making it possible for accurate localization through regression.

A. CSI Data Denoising

Observations show that raw CSI data have noise. Fig. 3(a) shows the raw CSI data collected from three receiving anten-
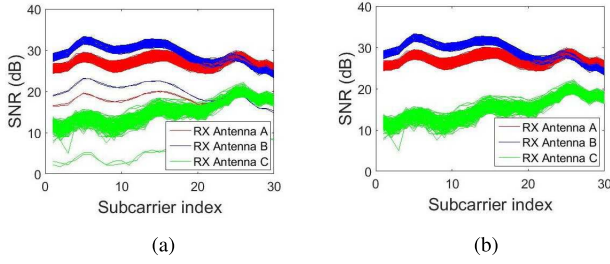
Fig. 3. CSI denoising with DBSCAN. (a) Raw CSI data. (b) Denoised CSI data.

nas in a MP, in which the isolated slim curves are noise. We apply the DBSCAN algorithm to detect and remove the noise. DBSCAN [24] is a density-based clustering algorithm, which groups points that are closely packed together and marks as outliers that lie alone in low-density regions. It does not require to specify the number of clusters a priori and can be used to detect and remove noise. DBSCAN is performed on the dataset of each TX-RX link. An AP-MP pair contains $N_{tx} \times N_{rx}$ TX-RX links with each link having N subcarriers. Thus, we divide the raw CSI dataset D into $N_{tx} \times N_{rx}$ data subsets, with each data subset D_{ij} representing a TX-RX link. A point in D_{ij} can be expressed as $o(k, v)$, where $k \in [1, N]$ represents the subcarrier index and v represents the CSI amplitude. After applying the DBSCAN denoising algorithm, as shown in Algorithm 1, the CSI data of the three links are shown in Fig. 3(b), which illustrates that the noise is removed effectively.

B. CSI Feature Extraction

Considering there are N_{ap} AP-MP pairs and each pair of AP-MP contains $N_{tx} \times N_{rx}$ links, and each link has N subcarriers, thus each CSI sample has $N_{ap} \times N_{tx} \times N_{rx} \times N$ dimensions. In our testbed in the research laboratory, a CSI sample contains 360 dimensions, while in the meeting room a CSI sample contains 270 dimensions. High dimensionality causes time complexity. As each dimension may have different contribution to presence detection and localization, we apply PCA algorithm to extract the most contributing features and reduce the dimensionality of CSI data. PCA [25] converts a set of possibly correlated variables into a set of linearly uncorrelated variables, called principal components, through orthogonal transformation. The first principal component has the largest possible variance, and each succeeding component in turn has the highest variance possible and orthogonal to the preceding components. For the goal of dimensionality reduction, PCA is to find l new features, with each one being a linear combination of the original features, so that the new features can reveal the nature of the original data and compress them. Through PCA on the CSI matrix H, we obtain the transformation matrix T, the transformed matrix S and the feature weights $W = (w_1, w_2, \cdots, w_L)$ in descending order, wherein L is the number of the original features. The cumulative contribution rate C_i till feature i is defined as

$$C_i = \frac{\sum_{j=1}^{i} w_j}{\sum_{j=1}^{L} w_j} \tag{5}$$

Algorithm 1: CSI Denoising With DBSCAN

Input: The data subset D_{ij};
Input: The neighborhood radius ε;
Input: The minimal number of points $minPts$;
Output: The denoised data subset D_{ij};
1: Mark all the points in D_{ij} as "unvisited";
2: **for** each point $o(k, v) \in D_{ij}$ **do**
3:     Mark $o(k, v)$ as "visited";
4:     Calculate Euclidean distance from points in D_{ij} to o;
5:     Calculate the ε-neighborhood of o;
6:     **if** (number_of_neighbors $\geq minPts$) **then**
7:         o is regarded as a core point;
8:         Mark all the neighbors as "visited";
9:         Create a new cluster C for o;
10:         Create a candidate set R for o;
11:         Put all the neighbors to candidate set R;
12:         **repeat**
13:             Pick a point p from candidate set R;
14:             **if** (p does not belong to other clusters) **then**
15:                 Put p in cluster C;
16:             **end if**
17:         **until** (candidate set R is empty)
18:         Cluster C is completed;
19:     **else**
20:         Label o as noise;
21:     **end if**
22: **end for**
23: The points labeled as noise are removed from D_{ij};
24: **return** D_{ij}.

If the cumulative contribution rate of the first l features, i.e. C_l, is greater than the predefined threshold C_c, we take the first l features, i.e. $(w_1, w_2, \cdots, w_l)$, as the extracted features. The first l rows of the transformed matrix S constitute the principal component matrix R, which will be used for the subsequent model training, presence detection and localization.

IV. PRESENCE DETECTION AND LOCALIZATION

Device-free presence detection aims to detect human presence in an area of interest without participation of mobile devices. It can be regarded as a binary classification problem, with one class as human presence and the other as vacancy. Device-free localization is to estimate the coordinates of the objects, without active participation of mobile devices as well. It can be solved as a regression problem by establishing the nonlinear dependency between locations and CSI fingerprints. SVM is an effective machine learning tool [26], which can be used for classification—Support Vector Classification (SVC) and regression—Support Vector Regression (SVR).

A. Presence Detection by SVM Classification

Classification consists of training and testing. Each training sample contains a class label and several features. Classification is to determine the labels of the testing samples according to their features, based on the models established

using the training samples. For the problem of presence detection, two kinds of CSI samples need to be collected during training: (1) positive samples collected with human presence; (2) negative samples collected when vacancy. Assume n is the number of training samples, l denotes the dimensionality of features. Each training sample consists of a pair (r_i, c_i), where $r_i = (r_{i1}, r_{i2}, \cdots, r_{il})$ is a vector representing the features, i.e. CSI fingerprints after DBSCAN and PCA, and $c_i \in \{-1, +1\}$ is the label assigned during training, with $+1$ representing human presence and -1 representing vacancy. These labeled samples are used to establish the SVM classifiers. Assume (r, c) is a testing sample, with $r \in R^l$ as the CSI fingerprint, classification is to determine the value of c, i.e. to determine human presence or vacancy in the area of interest.

The CSI fingerprints need to be normalized before classification, for higher precision and faster convergence. Normalization is performed on each individual feature. Let $r_{\min,j} = \arg\min_i r_{ij}$ represent the minimal value of the j-th feature, and $r_{\max,j} = \arg\max_i r_{ij}$ represent the maximal value of the j-th feature, the normalized value of r_{ij} is calculated as

$$r_{ij} = \frac{r_{ij} - r_{\min,j}}{r_{\max,j} - r_{\min,j}} \tag{6}$$

Using the normalized samples, we adopt C-SVC [26] for classification, which solves the following problem:

$$\text{minimize} \quad \frac{1}{2}\|w\|^2 + C\sum_{i=1}^{n}\xi_i$$

$$\text{subject to} \quad \begin{cases} c_i(w^T r_i + b) \geq 1 - \xi_i \\ C > 0, \quad \xi_i \geq 0 \end{cases} \tag{7}$$

where, $w \in R^l$ is a vector representing the direction of the separating hyperplane, $b \in R$ is a constant representing the location of the hyperplane, the constant C defines the tradeoff between a large separation region and misclassification errors, $\xi = (\xi_1, \xi_2, \cdots, \xi_n)$ are slack variables to allow some samples to be in the wrong side of the separating hyperplane. Solving equation (7) yields the classification function

$$f(r) = sign(\sum_{i=1}^{n} c_i \alpha_i K(r_i, r) + b) \tag{8}$$

where α_i is Lagrange multiplier, $K(r_i, r)$ is the kernel function mapping CSI fingerprints into a higher dimensional feature space. We choose RBF as the kernel function, which has the form of

$$K(x_i, x_j) = exp(-\gamma \|x_i - x_j\|^2) \tag{9}$$

with $\gamma > 0$ as the kernel parameter. $f(r) > 0$ indicates that a human appears in the area of interest, while $f(r) < 0$ indicates no human presence. Presence detection is a binary classification problem, requiring one classification model. Two parameters need to be trained for C-SVC: C and γ, which are determined by grid searching and cross-validation.

B. Localization by SVM Regression

For regression each training sample contains one target value and several features. Regression is to establish the

functional dependency between the features and the target values based on the training samples, and thus able to determine the target values of the testing samples according to their features. For the problem of localization, the target values are location coordinates and the features are CSI fingerprints after DBSCAN and PCA. Model training is to establish the functional dependency between CSI fingerprints and location coordinates. Assume n is the number of labeled training samples and l denotes the feature dimensionality. Each labeled sample consists of a pair $(r_i, (x_i, y_i))$, where $r_i \in R^l$ is a vector representing a CSI fingerprint after DBSCAN and PCA, $x_i \in R$ denotes the x-coordinate and $y_i \in R$ denotes the y-coordinate where r_i is measured. Model training is to establish the functional dependency f_x between CSI fingerprints and x-coordinates using the empirical dataset $\{(r_i, x_i)|i = 1, 2, \cdots, n\}$ and the functional dependency f_y between CSI fingerprints and y-coordinates using the empirical dataset $\{(r_i, y_i)|i = 1, 2, \cdots, n\}$. Assume $(r, (x, y))$ is a testing sample, with $r \in R^l$ representing the CSI fingerprint, localization is to determine x and y with f_x and f_y. Similar to normalization prior to SVC, the CSI fingerprints need to be normalized before SVR as well.

The standard form of SVR is ϵ-SVR [26]. Its goal is to find the function $f(r)$ that has at most ϵ deviation from the actually obtained target values c_i for all the training data $\{(r_1, c_1), (r_2, c_2), \cdots, (r_n, c_n)\} \subset R^l \times R$, c_i here represents the target values which are replaced by observed x_i for f_x regression and y_i for f_y regression. ϵ-SVR needs to specify the desired accuracy of approximation, i.e. ϵ, a priori. However, for localization, we expect the estimation to be as accurate as possible without having to commit ourselves to a specific level of accuracy a priori. Schölkopf et al. [27] introduced a new parameter $\nu \in (0, 1]$ and proposed ν-SVR, which automatically minimizes ϵ. The size of ϵ is traded off against model complexity and slack variables via the constant ν. We adopt ν-SVR, which solves the following problem:

$$\text{minimize} \quad \frac{1}{2}\|w\|^2 + C(\nu\epsilon + \frac{1}{n}\sum_{i=1}^{n}(\xi_i^* + \xi_i))$$

$$\text{subject to} \quad \begin{cases} (w^T r_i + b) - c_i \leq \epsilon + \xi_i \\ c_i - (w^T r_i + b) \leq \epsilon + \xi_i^* \\ \xi_i, \xi_i^*, \quad \epsilon \geq 0 \end{cases} \tag{10}$$

where, $w \in R^l$ is a vector representing the direction of the function, $b \in R$ is a constant representing its location, r_i is a CSI fingerprint, c_i is a coordinate dimension. For each sample an error of ϵ is allowed, everything above ϵ is captured by slack variables ξ_i and ξ_i^*, which are penalized via a regularization constant $C > 0$, chosen a priori. Solving equation (10) yields the function approximating the relationship:

$$f(r) = \sum_{i=1}^{n}(\alpha_i - \alpha_i^*)K(r_i, r) + b \tag{11}$$

where α_i and α_i^* are Lagrange multipliers, $K(r_i, r)$ is the kernel function using RBF. Two ν-SVR models need to be
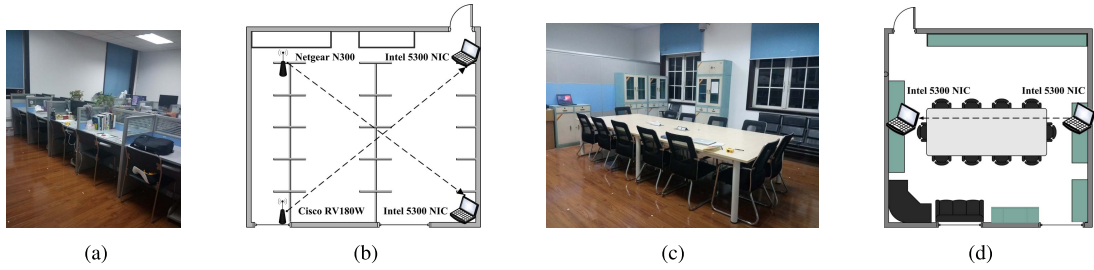
Fig. 4.   The testbeds: the research laboratory and the meeting room. (a) Laboratory. (b) Laboratory. (c) Meeting room. (d) Meeting room.
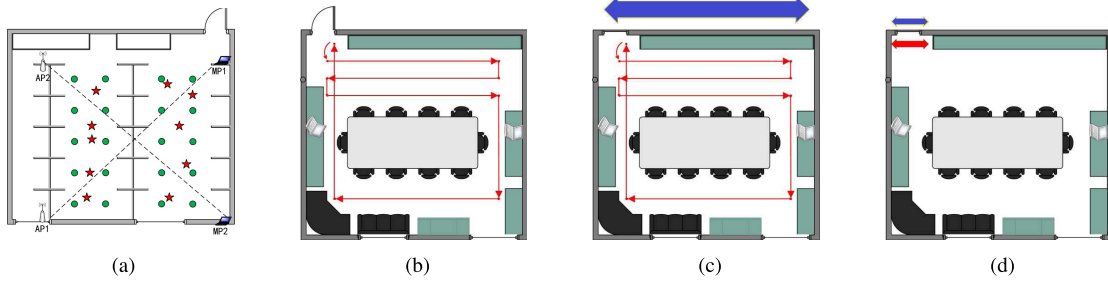

Fig. 5.   The testing settings for presence detection. Circles represent reference locations and stars represent testing locations. Lines are walking paths. (a) Laboratory. (b) Meeting room. (c) Meeting room. (d) Meeting room.

established, for x-coordinate and y-coordinate. Three parameters need to be trained for each v-SVR model: C, γ and v, which are determined by grid searching and cross-validation.

V. EVALUATIONS

A. Testing Setup

Experiments were conducted in our research laboratory (7 m×6 m) and meeting room (6 m×6 m). In the research laboratory, as shown in Fig. 4(a) and 4(b), we employed a Netgear N300 wireless router and a Cisco RV180W wireless router as transmitters, operating in IEEE 802.11n AP mode and in 2.4 GHz band, both having two transmitting antennas, and two computers equipped with Intel Wireless Link 5300 NICs (IWL5300) as receivers, each with three receiving antennas. The firmware and driver of IWL5300 are modified to export CSI of each packet [22], [23], which contains 30 groups of subcarriers. The two APs and two MPs were placed at the corners of the laboratory to cover the area. In the meeting room, we employed two computers, each equipped with IWL5300, one transmitting packets and the other receiving, working in 5GHz band, as shown in Fig. 4(c) and 4(d). The two computers were placed at the edges of the meeting room to cover the area.

B. Presence Detection

1) Data Collection: Presence detection were evaluated in the research laboratory and the meeting room separately, with five groups of testings, as Fig. 5 shows. Group A was to evaluate presence detection of a stationary human and Group B to E were to evaluate presence detection of a walking human. Group A of evaluations were conducted in the research laboratory, as shown in Fig. 5(a). During training, the testing volunteer traversed each of the 20 reference locations, marked as circles, and 50 samples were collected for each reference

location. 1000 samples were then collected when the laboratory was vacant. Thus, there were 1000 positive (presence) samples and 1000 negative (vacant) samples in the training set, which were used to establish the classifier of presence detection. For testing, 100 samples were collected during the volunteer standing at each of the 10 testing locations, marked as stars, and 1000 samples were collected when the laboratory was vacant. Thus 1000 positive testing samples and 1000 negative testing samples were prepared. Group B of evaluations were conducted in the meeting room. During training, 1000 samples were collected when the volunteer walked along the line marked in Fig. 5(b), and 1000 samples were collected when both the meeting room and the outside corridor were vacant. Thus the process produced 1000 positive and 1000 negative training samples. Collection of the testing samples followed the same process, producing 1000 positive and 1000 negative testing samples. Group C of evaluations were conducted in the meeting room as well, to investigate the influence of human walking on the outside corridor. 1000 negative training samples and 1000 negative testing samples were collected when the volunteer walked along the corridor outside the meeting room, as shown in Fig. 5(c). Group D of evaluations were also conducted in the meeting room, as shown in Fig. 5(d), to evaluate the detection performance in the door area. 1000 positive samples were collected when the volunteer walked along the line inside the door and 1000 negative samples were collected when the volunteer walked along the line outside the door, for training and testing, respectively. Group E merged the samples of group B, C and D, i.e. all the samples for the meeting room.

2) Results of Presence Detection: We employ five metrics to evaluate the performance of presence detection: (1) False Positive (FP) is the probability of failing to detect human presence; (2) True Positive (TP) equals to 1-FP; (3) False Negative (FN) is the probability of lying about human presence

TABLE I
RESULTS OF PRESENCE DETECTION WITH CSI AND SVC

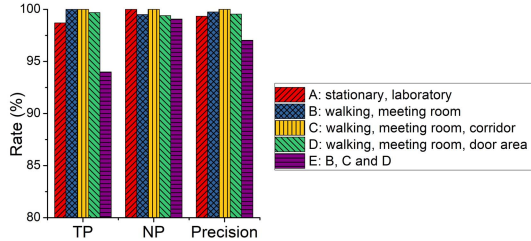| Testbed	Group	TP	FP	TN	FN	Precision
Lab	A	98.7%	1.3%	100%	0.0%	99.35%
	B	100%	0.0%	99.5%	0.5%	99.75%
Meeting	C	100%	0.0%	100%	0.0%	100.0%
	D	99.7%	0.3%	99.4%	0.6%	99.55%
	E (BCD)	94.0%	6.0%	99.1%	0.9%	97.04%

Fig. 6. Results of presence detection with CSI and SVC. Group A was in the research laboratory with human stationary. Groups B, C and D were in the meeting room with human walking. Group B was with the corridor vacant, while group C was with human walking on the corridor. Group D was in the door area. Group E merged the samples of B, C and D.

TABLE II
PRESENCE DETECTION WITH DIFFERENT METHODS

	Testbed	Method	FP	FN	Precision
CSI vs. RSSI	Lab	CSI	1.3%	0.0%	99.35%
		RSSI	15.8%	2.9%	90.65%
	Meeting	CSI	6.0%	0.9%	97.04%
		RSSI	54.7%	0.3%	77.98%
Feature extraction	Lab	PCA	1.3%	0.0%	99.35%
		SIED	5.0%	0.0%	97.50%
		R-TTWD	0.0%	5.0%	97.50%
	Meeting	PCA	6.0%	0.9%	97.04%
		SIED	5.0%	15.0%	91.00%
		R-TTWD	3.3%	20.0%	90.00%
SVC vs. BAY	Lab	SVC	1.3%	0.0%	99.35%
		BAY	1.8%	0.0%	99.10%
	Meeting	SVC	6.0%	0.9%	97.04%
		BAY	0.1%	41.8%	83.22%
Kernel	Meeting	RBF	6.0%	0.9%	97.04%
		Linear	3.0%	8.7%	94.76%
		Polynomial	2.6%	9.2%	94.78%
		Sigmoid	3.4%	12.4%	93.02%
Antenna	Meeting	1TX-1RX	20.3%	1.5%	91.00%
		2TX-2RX	3.7%	0.9%	98.00%
		3TX-3RX	6.0%	0.9%	97.04%

when no one appears; (4) True Negative (TN) equals to 1-FN; (5) Precision is the probability of detecting presence and vacancy correctly. The evaluation results of presence detection using the proposed method with CSI and SVC on the five groups of samples are listed in Table I and illustrated in Fig. 6. For all the tested groups, the method is able to achieve the detection precision of more than 97%, including the door area and the corridor, regardless of human stationary or walking. Performances of group A, B, C and D are comparable, achieving more than 99%, while group E is slightly worse as it merges the diverse samples from group B, C and D. In the research laboratory (group A) the method detects stationary human with 99.35%, and in the meeting room (group E) the method detects walking human with 97.04%.

3) Comparison and Analyses: We conducted presence detection testings with the common measurement RSSI in the same testbeds and compared them with the CSI-based approach. During the collection of CSI samples, we collected RSSI samples in parallel. The comparison of the results is reported in Table II. CSI outperformed RSSI by 24.4% in the meeting room and 9.6% in the research laboratory.

Extracted features are of key importance to the performance of presence detection. We implemented the feature extraction methods proposed by SIED [6] and R-TTWD [7] and compared them with our method using PCA, all followed with SVC to detect presence. SIED captured the variance of variances of amplitudes of each CSI subcarrier as features, while R-TTWD extracted first-order difference of eigenvector of CSI amplitudes across different subcarriers as features. The comparison of the three feature extraction methods is reported in Table II. Although the dimensionality of SIED (6 for laboratory, 9 for meeting room) and R-TTWD (18 for laboratory, 27 for meeting room) are lower than PCA (93 for laboratory, 48 for meeting room), PCA outperforms SIED and R-TTWD by 1.9% in the research laboratory, and outperforms SIED and R-TTWD by 6.6% and 7.8% in the meeting room.

Presence detection was evaluated with Bayesian algorithm (preceded by DBSCAN and PCA) as well, using the same training and testing sets. The comparison of the results is reported in Table II. Compared with Bayesian, SVC performed 0.25% better in the research laboratory and 16.6% better in the meeting room.

We chose RBF as the kernel function for SVC. To evaluate its performance, we compared it with other common kernel functions: linear, polynomial and sigmoid. The results in the meeting room are shown in Table II, which shows that RBF outperforms the other kernel functions by more than 2.4%.

To evaluate the effect of the number of antennas on the performance of presence detection, we randomly chose 1TX-1RX, 2TX-2RX, and 3TX-3RX, and conducted evaluations in the meeting room. The evaluation results are shown in Table II, which show that the presence detection precision can be enhanced by using multiple antennas. From 1TX-1RX to 2TX-2RX, the precision was improved by 7.7%, from 1TX-1RX to 3TX-3RX, the precision was improved by 6.6%, while the performances of 2TX-2RX and 3TX-3RX were comparable.

C. Device-Free Localization

1) Data Collection: Device-free localization were evaluated in the research laboratory and the meeting room separately, as Fig. 4 and Fig. 7 illustrate.

a) Laboratory: During training, the MPs collected raw CSI data from the connected APs during the volunteer standing at each reference location. The distribution of the 20 reference locations is shown in Fig. 7(a) as the circles, each having 100 samples. Testings were conducted at 10 testing locations, different from the reference locations, as the stars show in Fig. 7(a), each having 100 samples. As there are two AP-MP pairs in the research laboratory, each AP with two transmitting antennas and each MP with three receiving antennas, there are 12 links. Each link contains 30 groups of subcarriers,
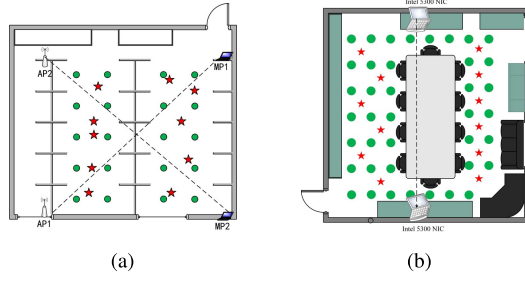
Fig. 7. The testing settings for device-free localization. Circles represent reference locations and stars represent testing locations. (a) Laboratory. (b) Meeting room.
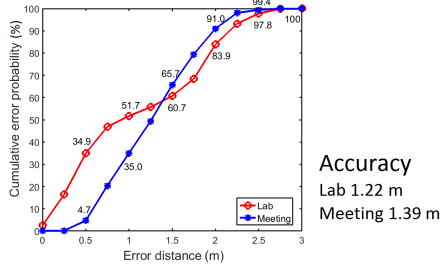

Fig. 8. Localization precision and accuracy with CSI and SVR.

TABLE III
LOCALIZATION ACCURACY OF DIFFERENT METHODS

	Method	Max.	Min.	Accuracy
DBSCAN	With	2.91 m	0.01 m	1.22 m
	Without	2.38 m	0.17 m	1.56 m
PCA	With	2.91 m	0.01 m	1.22 m
	Without	2.66 m	0.03 m	1.33 m
	RBF	2.91 m	0.01 m	1.22 m
Kernel	Linear	6.46 m	0.05 m	2.17 m
	Polynomial	2.96 m	0.42 m	1.83 m
	Sigmoid	5.26 m	0.24 m	2.16 m
SVR vs.	SVR	2.91 m	0.01 m	1.22 m
SVC vs.	SVC	3.87 m	0.34 m	2.03 m
BAY	BAY	3.87 m	0.24 m	2.10 m
	SVR-CSI	2.91 m	0.01 m	1.22 m
CSI vs.	SVR-RSSI	3.86 m	0.12 m	2.14 m
RSSI	SVC-CSI	3.87 m	0.34 m	2.03 m
	SVC-RSSI	4.53 m	0.34 m	2.56 m
SVR vs.	SVR	2.76 m	0.28 m	1.39 m
state of the art	MonoStream	2.00 m	1.00 m	1.64 m
	DeepFi	2.70 m	1.05 m	1.97 m

thus a CSI sample has 360 dimensions. After denoising by DBSCAN and dimensionality reduction by PCA, 93 features were extracted and constituted a CSI fingerprint, achieving the cumulative contribution rate of more than 99%.

b) Meeting room: Circles in Fig. 7(b) show the distribution of the 40 reference locations in the meeting room, each having 100 samples. Testings were conducted at 12 testing locations, as the stars show in Fig. 7(b), each having 100 samples. As one AP-MP pair was employed in the meeting room, each AP with three transmitting antennas and each MP with three receiving antennas, there are 9 links, thus a CSI sample has 270 dimensions. After denoising and dimensionality reduction, 48 features were extracted and constituted a CSI fingerprint, achieving the cumulative contribution rate of more than 99%.

2) Results of Localization: We conducted device-free localization experiments with CSI through SVR. Two metrics are used to analyze the localization performance: (1) Accuracy represents the mean error distance; (2) Precision represents the cumulative error probability. The localization results with CSI and SVR in the research laboratory and the meeting room are shown in Fig. 8. In the research laboratory, the accuracy is 1.22 m, and the minimal and the maximal error distances are 0.01 m and 2.91 m, respectively. The error distance is within 1 m with the probability of 51.7%, within 2 m 83.9%, and within 3 m 100%. In the meeting room, the accuracy is 1.39 m, and the minimal and the maximal error distances are 0.28 m and 2.76 m, respectively. The error distance is within 1 m with the probability of 35.0%, within 2 m 91.0%, and within 3 m 100%. We carried out further evaluations in a larger environment of two rooms with the size of 6 m × 16 m using one pair of AP-MP, with 59 reference locations

and 30 testing locations. The accuracy achieved is 1.77 m, and the minimal and the maximal error distances are 0.03 m and 4.24 m. The error distance is within 1 m with the probability of 28.5%, within 2 m 60.4%, and within 3 m 85.5%.

3) Denoising and Feature Extraction: Testings were made in the research laboratory to evaluate the effect of the data denoising method. The localization results with and without DBSCAN denoising are shown in Table III. The accuracy with DBSCAN is better than without DBSCAN by 0.34 m, which is a gain of 21.8%. The comparison between the precision of them are shown in Fig. 9(a), in which SVR with DBSCAN outperforms without DBSCAN.

The algorithm applies PCA to extract the features and reduce the dimensionality of CSI fingerprints. By setting a cumulative contribution rate of 99%, the dimensionality in the research laboratory was reduced from 360 to 93, and the regression time of one testing reduced from 2.58 ms to 0.45 ms. The localization results with and without PCA in the research laboratory are shown in Table III. The accuracy with PCA is better than without PCA by 0.11m, a gain of 8.3%. The comparison between the precision of them are shown in Fig. 9(b), in which SVR with PCA outperforms without PCA.

4) Comparison and Analyses: We chose RBF as the kernel function for SVR. We also carried out localization experiments in the research laboratory with other common kernel functions: linear, polynomial and sigmoid. The comparisons are shown in Table III and Fig. 9(c), in which RBF outperforms the other kernel functions by more than 30%.

State of the art applies Bayesian [2], [3] or classification algorithms [8], [9] to perform CSI fingerprinting. Therefore, we made localization testings with Bayesian and SVC (both preceded with DBSCAN and PCA) in the research laboratory, for the purpose of comparison. The results of them are shown in Table III. The accuracy of SVC and Bayesian are almost equal, 2.03 m and 2.10 m, respectively, around 40% worse than SVR. The comparison of precision of them is shown in Fig. 9(d), in which SVR outperforms SVC and Bayesian by a large margin. The major reason is that localization is a continuous problem instead of a discrete one, thus the
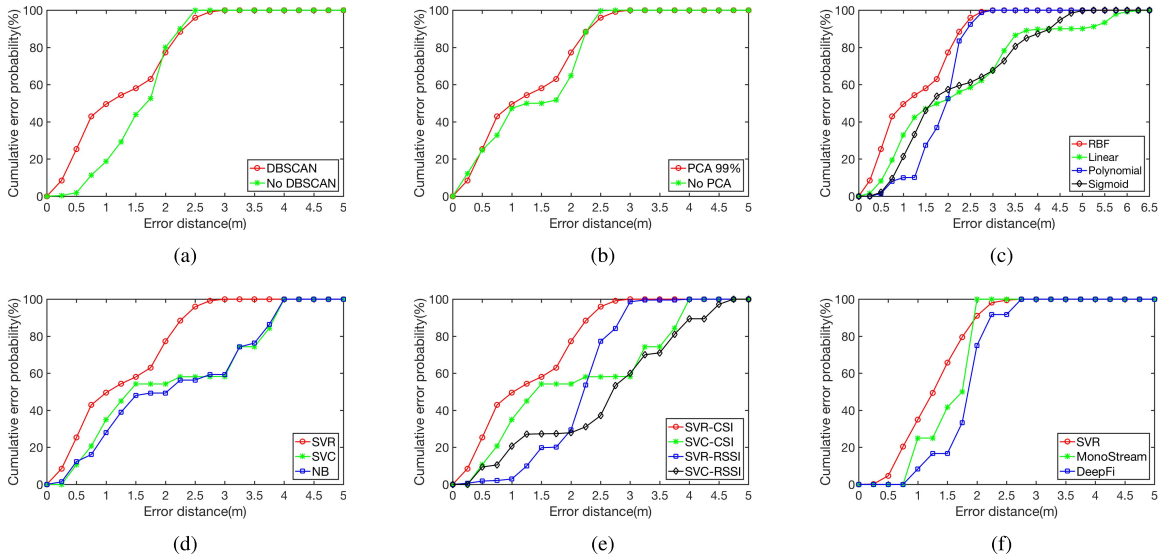
Fig. 9. Localization precision of different methods. (a) DBSCAN. (b) PCA. (c) Kernel function. (d) SVR vs. SVC vs. BAY. (e) CSI vs. RSSI. (f) SVR vs. state of the art.

regression algorithm SVR suits more appropriately than SVC and Bayesian.

To compare the performance of CSI with commonly used RSSI, we carried out localization experiments with RSSI using SVC and SVR in the research laboratory. The evaluation results are reported in Table III and Fig. 9(e). The results show that no matter using SVC or SVR, the CSI approach outperforms the RSSI approach significantly, by 43.0% using SVR and 20.7% using SVC. SVR outperforms SVC by 40.0% with CSI and by 16.4% with RSSI.

We compared our work to the state of the art MonoStream [9] and DeepFi [8]. MonoStream [9] adopted an object recognition solution in a device-free manner while DeepFi utilized a deep learning approach in a device-based manner. We conducted passive localization experiments with the three solutions using the same datasets in the meeting room. The results show that our solution outperforms MonoStream and DeepFi wrt. localization accuracy and precision, as illustrated in Table III and Fig. 9(f). Our solution outperforms MonoStream by 15.2% and outperforms DeepFi by 29.4% wrt. accuracy. The comparison demonstrates the effectiveness of DBSCAN+PCA+SVR on localization. As for the computing time, when running on a computer with Intel Core i5–4460 3.20GHz and 8G RAM, our solution spent 4 ms for one localization, while DeepFi took 15 ms and MonoStream took 65 ms for one localization.

5) Effect of Parameters on Localization: We carried out testings to investigate the effect of parameters on localization. We tested two pairs of AP-MP, one pair of AP-MP using the Cisco router, the Netgear router, and the IWL5300 in AP mode. The localization results are shown in Table IV and Fig. 10(a). One pair of AP-MP is able to provide acceptable localization performance, while two pairs of AP-MP achieve better accuracy, as more links provide better coverage and more features. Different types of routers exhibit different localization capability. We randomly chose 1TX-1RX and 2TX-2RX, and compared with 2TX-3RX. The evaluation

TABLE IV
LOCALIZATION ACCURACY WRT. PARAMETERS

Parameter	Value	Max.	Min.	Accuracy
AP-MP pairs	2	2.91 m	0.01 m	1.22 m
	1 Cisco	3.16 m	0.19 m	1.33 m
	1 Netgear	3.72 m	0.37 m	1.50 m
	1 IWL5300	2.76 m	0.28 m	1.39 m
Antenna numbers	2TX-3RX	2.91 m	0.01 m	1.22 m
	2TX-2RX	3.44 m	0.02 m	1.33 m
	1TX-1RX	2.51 m	0.03 m	1.61 m
Ref. location numbers	20	2.91 m	0.01 m	1.22 m
	12	3.19 m	0.04 m	1.38 m
	6	2.64 m	0.06 m	1.60 m
Cumulative contribution rate	93%	3.68 m	0.00 m	1.57 m
	95%	3.08 m	0.01 m	1.47 m
	97%	2.53 m	0.05 m	1.34 m
	99%	2.91 m	0.01 m	1.22 m
	100%	2.66 m	0.03 m	1.33 m

results in the research laboratory are shown in Table IV and Fig. 10(b), which show that the localization accuracy can be enhanced by using more antennas. From 1TX-1RX to 2TX-2RX, the localization accuracy is improved by 17.4%; from 2TX-2RX to 2TX-3RX, it is further improved by 8.3%. We tested three sampling densities, 20, 12 and 6 reference locations in the research laboratory. Table IV and Fig. 10(c) show that with the increase of the number of reference locations, i.e. with the increase of sampling density, the localization accuracy grows. When the number of reference locations increases from 6 to 12, the accuracy improves 13.8%, and when the number increases to 20, the accuracy improves further 11.6%. We investigated the effect of the cumulative contribution rate C_c by setting it as 93%, 95%, 97%, 99% and 100% (i.e. without PCA). Results in Table IV and Fig. 10(d) show that with the increase of C_c, the localization accuracy grows, 99% achieves the best accuracy, even better than 100%. Meanwhile, the feature dimensionality and regression time grow with C_c. The regression time of one sample for $C_c = 99\%$ is 0.45 ms, which is acceptable and much shorter than $C_c = 100\%$.
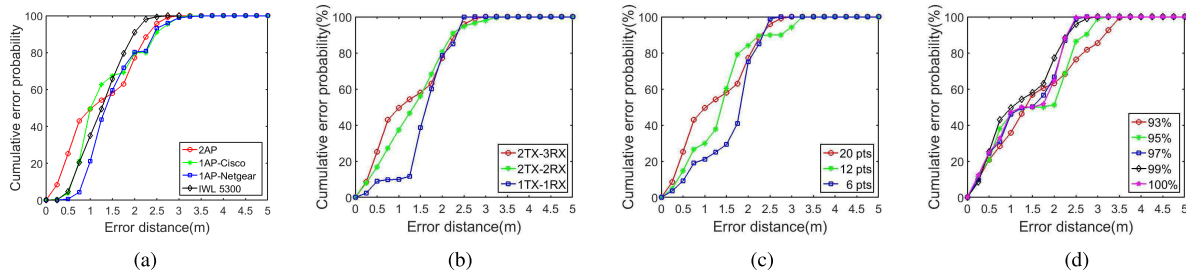
Fig. 10. Localization precision wrt. parameters. (a) Number of AP-MP pairs. (b) Number of antennas. (c) Number of reference locations. (d) Cumulative contribution.

VI. CONCLUSIONS

OFDM and MIMO make it possible to access fine-grained physical channel frequency response of multiple links, thus trigger the use of CSI to achieve more accurate device-free presence detection and localization. This paper presents a CSI-based device-free presence detection and localization algorithm, by applying SVC to solve the presence detection problem through classification and applying SVR to solve the localization problem through regression. DBSCAN is applied on CSI data to reduce noise and PCA is applied to extract features and reduce dimensionality. Evaluations prove the effectiveness of the algorithm, achieving localization accuracy of 1.22 m in the research laboratory and 1.39 m in the meeting room, and presence detection precision of more than 97%.

REFERENCES

[1] K. Wu, J. Xiao, Y. Yi, M. Gao, and L. M. Ni, "FILA: Fine-grained indoor localization," in *Proc. IEEE INFOCOM*, Mar. 2012, pp. 2210–2218.

[2] H. Abdel-Nasser, R. Samir, I. Sabek, and M. Youssef, "MonoPHY: Mono-stream-based device-free WLAN localization via physical layer information," in *Proc. IEEE WCNC*, Apr. 2013, pp. 4546–4551.

[3] K. Wu, J. Xiao, Y. Yi, D. Chen, X. Luo, and L. M. Ni, "CSI-based indoor localization," *IEEE Trans. Parallel Distrib. Syst.*, vol. 24, no. 7, pp. 1300–1309, Jul. 2013.

[4] Z. Zhou, Z. Yang, C. Wu, L. Shangguan, and Y. Liu, "Omnidirectional coverage for device-free passive human detection," *IEEE Trans. Parallel Distrib. Syst.*, vol. 25, no. 7, pp. 1819–1829, Jul. 2014.

[5] C. Wu, Z. Yang, Z. Zhou, X. Liu, Y. Liu, and J. Cao, "Non-invasive detection of moving and stationary human with WiFi," *IEEE J. Sel. Areas Commun.*, vol. 33, no. 11, pp. 2329–2342, Nov. 2015.

[6] J. Lv, W. Yang, L. Gong, D. Man, and X. Du, "Robust WLAN-based indoor fine-grained intrusion detection," in *Proc. IEEE GLOBECOM*, Dec. 2016, pp. 1–6.

[7] H. Zhu, F. Xiao, L. Sun, R. Wang, and P. Yang, "R-TTWD: Robust device-free through-the-wall detection of moving human with WiFi," *IEEE J. Sel. Areas Commun.*, vol. 35, no. 5, pp. 1090–1103, May 2017.

[8] X. Wang, L. Gao, S. Mao, and S. Pandey, "CSI-based fingerprinting for indoor localization: A deep learning approach," *IEEE Trans. Veh. Technol.*, vol. 66, no. 1, pp. 763–776, Jan. 2017.

[9] I. Sabek and M. Youssef, "MonoStream: A minimal-hardware high accuracy device-free WLAN localization system," *Comput. Sci.*, 2013.

[10] J. Wang *et al.*, "LiFS: Low human-effort, device-free localization with fine-grained subcarrier information," in *Proc. MobiCom*, 2016, pp. 243–256.

[11] X. Li, S. Li, D. Zhang, J. Xiong, Y. Wang, and H. Mei, "Dynamic-MUSIC: Accurate device-free indoor localization," in *Proc. ACM UbiComp*, 2016, pp. 196–207.

[12] K. Qian, C. Wu, Z. Yang, C. Yang, and Y. Liu, "Decimeter level passive tracking with WiFi," in *Proc. HotWireless*, 2016, pp. 44–48.

[13] Y. Wang, J. Liu, Y. Chen, M. Gruteser, J. Yang, and H. Liu, "E-eyes: Device-free location-oriented activity identification using fine-grained WiFi signatures," in *Proc. 20th Annu. Int. Conf. Mobile Comput. Netw.*, 2014, pp. 617–628.

[14] K. Qian, C. Wu, Z. Zhou, Y. Zheng, Z. Yang, and Y. Liu, "Inferring motion direction using commodity Wi-Fi for interactive exergames," in *Proc. ACM CHI*, 2017, pp. 1961–1972.

[15] C. Han, K. Wu, Y. Wang, and L. M. Ni, "WiFall: Device-free fall detection by wireless networks," in *Proc. IEEE INFOCOM*, Feb. 2014, pp. 271–279.

[16] H. Wang, D. Zhang, Y. Wang, J. Ma, Y. Wang, and S. Li, "RT-Fall: A real-time and contactless fall detection system with commodity WiFi devices," *IEEE Trans. Mobile Comput.*, vol. 16, no. 2, pp. 511–526, Feb. 2017.

[17] H. Li, W. Yang, J. Wang, Y. Xu, and L. Huang, "WiFinger: Talk to your smart devices with finger-grained gesture," in *Proc. UbiComp*, 2016, pp. 250–261.

[18] W. Wang, A. X. Liu, and M. Shahzad, "Gait recognition using WiFi signals," in *Proc. UbiComp*, 2016, pp. 363–373.

[19] W. Xi *et al.*, "Electronic frog eye: Counting crowd using WiFi," in *Proc. IEEE INFOCOM*, Apr. 2014, pp. 361–369.

[20] S. D. Domenico, G. Pecoraro, E. Cianca, and M. D. Sanctis, "Trained-once device-free crowd counting and occupancy estimation using WiFi: A Doppler spectrum based approach," in *Proc. IEEE WiMob*, Oct. 2016, pp. 1–8.

[21] R. Zhou, J. Chen, X. Lu, and J. Wu, "CSI fingerprinting with SVM regression to achieve device-free passive localization," in *Proc. IEEE WoWMoM*, Jun. 2017, pp. 1–9.

[22] D. Halperin, W. Hu, A. Sheth, and D. Wetherall, "Predictable 802.11 packet delivery from wireless channel measurements," in *Proc. ACM SIGCOMM*, 2010, pp. 159–170.

[23] *Linux 802.11n CSI Tool*. Accessed: Aug. 10, 2017. [Online]. Available: http://dhalperi.github.io/linux-80211n-csitool/index.html#overview

[24] M. Ester, H.-P. Kriegel, J. Sander, and X. Xu, "A density-based algorithm for discovering clusters in large spatial databases with noise," in *Proc. KDD*, 1996, pp. 226–231.

[25] I. Jolliffe, *Principal Component Analysis*, 2nd ed. New York, NY, USA: Springer, 2002.

[26] T. Hastie, R. Tibsirani, and J. Friedman, *The Elements of Statistical Learning*, 2nd ed. New York, NY, USA: Springer, 2008.

[27] B. Schölkopf, A. J. Smola, R. C. Williamson, and P. L. Bartlett, "New support vector algorithms," *Neural Comput.*, vol. 12, no. 5, pp. 1207–1245, 2000.

Rui Zhou received the Ph.D. degree from the University of Freiburg, Germany, in 2010. She is currently an Associate Professor with the University of Electronic Science and Technology of China. Her research interests include pervasive computing and machine learning.

Xiang Lu is currently pursuing the master's degree with the University of Electronic Science and Technology of China. His research interests include localization and pervasive computing.

Pengbiao Zhao is currently pursuing the bachelor's degree with the University of Electronic Science and Technology of China. His research interests include localization and pervasive computing.

Jiesong Chen is currently pursuing the master's degree with the University of Electronic Science and Technology of China. His research interests include localization and Internet of Things.